Title:

A novel flexible capacitive load sensor for use in a mobile unicompartmental knee replacement bearing: an *in vitro* proof of concept study

Authors:

Mentink M J A, michielmentink@gmail.com, Nuffield Dept. of Orthopaedics, Rheumatology & Musculoskeletal Sciences, University of Oxford, Botnar Research Centre, Oxford, OX3 7LD, UK

Van Duren, B H, b.h.vanduren@gmail.com, Nuffield Dept. of Orthopaedics, Rheumatology & Musculoskeletal Sciences, University of Oxford, Botnar Research Centre, Oxford, OX3 7LD, UK

Murray D W, david.murray@ndorms.ox.ac.uk, Nuffield Dept. of Orthopaedics, Rheumatology & Musculoskeletal Sciences, University of Oxford, Botnar Research Centre, Oxford, OX3 7LD, UK

Gill H S, r.gill@bath.ac.uk, Department of Mechanical Engineering, University of Bath, Bath, BA2 7AY, UK

Corresponding author: michielmentink@gmail.com

Keywords

Tibiofemoral forces, capacitive load sensor, in vitro, load measurement, UHMWPE mechanical behaviour, flexible sensor, polyimide.

Acknowledgements

Biomet (Biomet UK Ltd, Swindon, UK) helped with compression moulding of the instrumented bearings.

Competing interests

One of the authors (DWM) receives royalty and consultancy payments related to unicompartmental knee replacement.

Funding:

This work was supported by an NIHR Senior Investigator Award made to Professor David Murray, April 2009 - March 2013.

Ethical approval:

Not required

Abstract

Instrumented knee replacements can provide *in vivo* data quantifying physiological loads acting on the knee. To date instrumented mobile unicompartmental knee replacements (UKR) have not been realised. Ideally instrumentation would be embedded within the polyethylene bearing. This study investigated the feasibility of an embedded flexible capacitive load sensor. A novel flexible capacitive load sensor was developed which could be incorporated into standard manufacturing of compression moulded polyethylene bearings. Dynamic experiments were performed to determine the characteristics of the sensor on a uniaxial servo-hydraulic material testing machine. The instrumented bearing was measured at sinusoidal frequencies between 0.1 and 10 Hz, allowing for measurement of typical gait load magnitudes and frequencies. These correspond to frequencies of interest in physiological loading. The loads that were applied were a static load of 390 N, corresponding to an equivalent body weight load for UKR, and a dynamic load of ±293 N**.** **The frequency transfer response of the sensor suggests a low pass filter response with a -3dB frequency of 10 Hz.** The proposed embedded capacitive load sensor was shown to be applicable for measuring *in vivo* loads within a polyethylene mobile UKR bearing.

1 Introduction

Mechanical loads experienced by human joints during functional activities play an important role in the initiation and progression of osteoarthritis (OA) resulting in joint degeneration [1, 2]. The ability to measure the loads that occur within joints *in vivo* can give a valuable insight into the disease process. Measuring joint loads *in vivo* presents many challenges; both technologically and ethically.

Previously studies have attempted to estimate the mechanical forces and moments in the knee from external gait measurements [3], mechanical simulations (*in vitro* assessment) [4], computer simulations [5, 6], and telemetered implants. However, these methods have shortcomings. Force calculations from external gait measurements are subject to a large number of assumptions. The accuracy of simulations is dependent on the data provided by measurements, for instance from telemetered implants [6]. Forces measured *in vivo* using those implants are reported to be lower than those calculated by models [7].

In recent decades, instrumented Total Knee Replacement (TKR) implants have been successfully used to measure joint loading. In TKR many of the important structures of the knee, such as the cruciate ligaments, are removed during surgery resulting in a significant change in the kinematics of the knee. Instrumented TKR implants may require additional bone volume to be removed in order to accommodate the added volume of the instrumentation [8-10]. In contrast during Unicompartmental Knee Replacement (UKR) most of the structures are left intact, particularly the cruciate ligaments, resulting in kinematics that more closely represent those of the normal knee [10-15].

Instrumentation of UKR potentially offers valuable data describing the loads experienced in the knee. To our knowledge an instrumented Unicompartmental Knee Replacement (UKR) has not

been developed. With UKR it is important to retain as much bone as possible. Therefore, the electronics need to be fitted within the implant components without requiring the removal of additional knee structures.

In the Oxford mobile bearing UKR (ZimmerBiomet Ltd, Swindon, UK), the majority of the load is perpendicular to the tibial tray, owing to the bearing being mobile in the transverse and sagittal planes. Therefore, embedding a sensor within the bearing may offer the least intrusive method of measuring load. Strain gauges have been used to measure forces in TKR implants. However, previous work suggested that stress levels within an Oxford UKR bearing could rise as high as 5 MPa [16], which translates to 0.015 strain. Given that the fatigue life of typical Constantan strain gauges falls below 10^5 cycles for strains of ±0.002 [17], using strain gauges to measure UHMWPE deformation directly would result in an unacceptably short sensor life, compared to the 16×10^6 loading cycles typically experienced by a UKR [16].

Capacitive sensors suffer less from a limited life span as the material under load can more readily be chosen to be able to withstand load. Additionally, insertion of components with an elastic modulus that is dissimilar to UHMWPE may cause stress risers and promote damage of the bearing [16] , whereas capacitive sensors can be designed to be more compliant, because sensor materials and electrode construction can be adjusted to closely match the mechanical properties of the host component. Polymer based capacitive sensors have previously been used to measure forces [18-25] but never to measure forces within joints and they have never been incorporated into industrial production process used in producing polyethylene bearings.

The aim of the current study was to investigate the feasibility of using a capacitive load sensor embedded in an existing design of a mobile bearing used in a UKR implant in order to measure loads acting on the knee. The minimum design specification for the sensor was that it should be able to measure static load equivalent to one body weight during one leg stance, which was defined as 780 N. The distribution of load between the condyles has been considered to have a

50/50 medial to lateral distribution [26-28], resulting in a static load of 390 N to be measured. Furthermore, the sensor should be able to measure a maximum expected frequency content of 4.2 Hz [29]; we therefore choose to use a conservative measurement frequency of 10 Hz. The sinusoidal load was set to be ± 75 % or ±293N of the static load, to prevent lift-off of the actuator at minimum load during testing. The specification for physical dimensions required the sensor to fit within the existing Oxford UKR bearing, giving a maximum size of 5 x 5 x 0.2 mm.

The construction of the UKR bearing with an embedded capacitive load sensor is detailed followed by *in vitro* tests to determine the characteristics of the capacitive load sensor embedded within a polyethylene UKR bearing.

2 Methods

Instrumented Bearing Design & Construction:

The Oxford UKR uses a fully conforming mobile bearing resulting in the predominant load being in the proximal-distal orientation normal to the tibial plateau. Therefore a capacitive sensor, consisting of parallel plates, placed within the centre of the bearing was designed.

The capacitance of two parallel plates can be calculated using the equation (*equation 1*):

Equation 1

$$C = \frac{\varepsilon_o * \varepsilon_r * A}{d}$$

where: capacitance, ε0 = permittivity of free space, 8.85e-12 F/m, εr = relative dielectric constant, A = overlapping area of two parallel electrodes [m^2], d = distance between electrodes [m]

When a load is applied to the sensor, the separation of the plates decreases, hence the capacitance increases. A sensor was developed which consisted of three copper layers (*Figure 1, Figure 2*), of which the outer two layers were electrically connected, resulting in a doubling of capacitance with respect to *Equation 1*, and providing shielding of the sensitive inner electrodes from electromagnetic interference by the common driven electrodes. The middle layer consisted of four electrodes (each with dimensions 2x2 mm) with an in-plane electrode separation of 0.5 mm. On the outer layers, there was a 5x5 mm common electrode. Together they formed four individually addressable capacitors. Polyimide (PI), a commonly used material for making flexible electronic circuits, was used for the dielectric layer. The total thickness of the sensor was 111 µm. The distance d between the electrodes was 44 µm, the area A of one electrode was 4E-6 m^2. The

capacitive sensor was kept small, primarily to retain as much of the mechanical integrity of the UHMWPE as possible, and secondarily to remain within the bounds of the maximum capacitance that the chosen Capacitive to Digital converter (C2D, AD7746 v2.2.2 Analog Devices Inc, Norwood, MA, USA) could measure. The capacitance of each electrode was measured to be nominally 16 pF, including the measurement leads *(Figure 3)*. The flexible capacitive force sensor printed circuit board was designed using the OrCAD 16.5 (Cadence Design Systems, San Jose, CA, USA). The sensors, designed by MM, were manufactured by Sunsoar Tech (Sunsoar Tech, Shenzhen, China), using standard Polyimide material 'SYE'. The C2D was used to send a signal to the common electrode and the electrode with the strongest load response was connected to the input of the C2D. This design was chosen because of its small size and potential for possible application in a future production instrumented knee replacement bearing.

In order to be able to embed the sensor directly under the centre of the bearing concavity, the flexible sensor was shaped with limbs to position the electrodes in the middle of the bearing (*Figure 3a*) during the moulding process. The sensor leads were folded in a harmonica-like manner so as to enable their release after the moulding process had been completed. The first step in the moulding process was to place a layer of half the required amount of UHMWPE powder in the bottom of the moulding tool for the UKR bearing. The sensor was then placed on top of this layer (*Figure 3b*), and the remaining UHMWPE powder added. With the mould filled, the normal production temperature and pressure profiles were used to mould the bearing (*Figure 3c*) [30]. Using a hot cutting tool, the UHMWPE covering the folded sensor lead was removed, and the lead was extended (*Figure 3d*). After that, the shielded connecting leads were soldered to each sensor lead for measurement. Five instrumented left sided, large, size 6, Phase 3, Oxford UKR knee bearings were made. The length and the width of the bearings were approximately 36x24 mm. The distance from the bottom of the bearing to the lowest point of the bearing concavity was 6.5 mm.

Sensor Testing:

In order to calibrate a given sensor, measurement of the linear load response to an increasing load is considered the gold standard [31]. However, UHMWPE is a polymer with viscoelastic properties [30, 32] resulting in the response under load being time dependent. With continuous compressive loads there is a gradual viscous response and for dynamic loads a rapid elastic response. A simplified representation of loading was utilized to compensate for the viscous response of UHMWPE: Loading of the knee joint can be considered to be the sum of two loading components: static loading resulting from gravitational force, and superimposed dynamic loading during dynamic gait activities. Pre-loading of a material, representing the gravitational force, minimizes the viscous response resulting in a predominantly linear response to dynamic loads experienced during the gait cycle.

To characterize the static and dynamic responses of UHMWPE, two experiments were conducted:
1) Initial pre-loading of UHMWPE to measure the duration of the viscous response to a step change in loading
2) Successive application of sinusoidal frequencies superimposed on the static pre-load in order to measure linearity of the system response.
These experiments were conducted using: a) A set of naked (unembedded) sensors (n=5) and b) A set of UKR bearings with the sensor embedded (n=5).

The experiments were designed to address the following questions:

- How long should a static load be applied before the viscous response is sufficiently reduced so as not to influence the dynamic measurements?
- What is the frequency response of the embedded load sensor?

- What distortion components are introduced to the measured signal?

A uniaxial servo-hydraulic material testing machine (Dartec DC10, Zwick, Leominster, UK) controlled by TIAB software version SR2 v2.06.17 (TIAB ltd, Middleton Cheney, UK) was used to apply loads. Load data were sampled at 100 Hz, using a load cell (DSCRCM-15KN, Zwick, Leominster, UK, calibrated to 10 kN, resolution 0.5 N). Compression was measured with the built-in Dartec LVDT. For C2D measurement, the AD7746 demonstration kit (Analog Devices Inc, Norwood, MA, USA), was used, and the accompanying software was adjusted 1) to automatically apply a capacitance offset at the onset of the measurement using the built in CAPDAC (a programmable static capacitive offset) of the AD7746 to enable measurement of large capacitance values, 2) to log data with time stamps, and 3) to measure at 90 samples per second. Room temperature was monitored by an external thermocouple temperature sensor (SE002 Type K, Pico Tech, Eaton Socon, UK).

To test the naked sensors 5x5x5 mm glass cubes were bonded to five sensor foils with a poly-acrylate adhesive and mounted in the servo-hydraulic testing machine. The glass cubes provided a separation of the metal actuator of the testing machine from the electrodes and ensured that load was applied only to the electrode surface area. For the UKR bearing with embedded sensors, loads were applied using a stainless steel component with the same radius and width as a large UKR femoral component (Biomet UK Ltd, Swindon, UK), mounted in the servo-hydraulic testing machine (*Figure 4*).

Testing was conducted according to the protocol below:

1) 10 minutes warm up of all equipment before start of experiment
2) Adjustment of C2D input range, using the built-in capacitive offset of the C2D
3) Start of measurement, record unloaded capacitance

4) Static load applied for 15 minutes to approach creep equilibrium (pre-loading). The total static knee load due to gravity was assumed to be 780 N, and the maximum static load on the medial side of the knee was approximated as being 50% [26-28], or 390 N.
5) Sinusoidal loading applied (frequency response measurements, see further details below)
6) Unloaded rest interval of 15 minutes

The above testing protocol was repeated five times per sensor/bearing (as previously mentioned n=5 for both naked sensors and instrumented bearings).

Frequency Response Measurements: The maximum signal frequency was determined to be 10 Hz based on Fourier analysis of *in vivo* gait and step up/down measurements obtained from www.orthoload.com [29]. Sinusoidal loading frequencies from 0.1 to 1 Hz in steps of 0.1 Hz and 1 to 10 Hz in steps of 1 Hz were applied to the test setup, each for 10 seconds, and the sensor output was measured. Frequencies lower than 0.1 Hz were not measured due to time constraints. A static load of 100 N and a dynamic sine wave load of ±33 N peak amplitude were applied to the upper glass cube for the naked sensor setup and a static load of 390 N with a dynamic sine wave of ± 293 N amplitude were applied to the UKR bearings embedded with the prototype sensor. A single sine model was fitted to both the measured loads and the resulting capacitance; the resulting fitted load amplitude was used to normalize the capacitance amplitude, in order to compensate for minor variations in loading amplitude.

Harmonic Distortion Analysis: Harmonic distortion analysis reveals the generation of higher order frequency components. Harmonic distortion was analysed using the normalised data that was used for the frequency response. To measure the harmonic distortion for each frequency (generation of higher harmonic frequencies), a dual sine wave model was fitted to the normalized measurement data.

237

238 *Sensitivity Calculation:* In order to compare the results with other work [19], the sensitivity (F/N)
239 was calculated, as well as the stress sensitivity (F/MPa), using a load of 33 N, and a surface
240 area of 2.5 X 10^{-5} m^2 (from [5x10^{-3}]^2).

241 All analyses were performed using custom scripts written in Matlab 8.2 (R2013b) (The
242 mathworks Inc, Natick, Massachusetts, USA)

3 Results

For all sensors the capacitance increased as load was increased, cycling the load led to a cycling of the capacitance values tracking the load. *Figure 5* provides an exemplar plot of the measured capacitance with time graph for a single test, showing the resulting loading pattern with an initial static pre-load and subsequent sine loading at various frequencies, and finally followed by the unloading phase for the embedded sensor.

A typical pre-loading change in capacitance with time for the naked sensor is shown in *Figure 6a* and the average change in capacitance over time for all five samples with five repeats per sample in *Figure 6b*. The results showed that after application of a fixed load for five to ten seconds, the sensor capacitance was within 5% of the capacitance value that was measured at the end of the experiment. A similar sensor response pattern was seen from the sensor embedded in the UKR bearing (*Figures 7a & 7b*). In the case of the embedded sensor the measured capacitance reached to within 5% of the capacitance value measured at the end of the experiment.

The mean value of the bare sensor capacitance varied by 10% over the frequency range 0.1 to 10 Hz (*Figure 8*). The median of the normalized capacitive amplitude change was $2 * 10^{-15} F$ [99.3 % CI: $0.67 - 8$], when stimulated with 33 N (*Figure 8*). This yielded a medium sensitivity of $6.1 * 10^{-17}$ F/N [99.3 % CI: $2.0 - 24$], and a stress sensitivity of $4.5 * 10^{-17}$ F/MPa [99.3 % CI $1.5 - 18$]. The amplitude fitted when with the single sinusoidal model was within -3 dB for all frequencies up to 10 Hz for both the naked sensor and the sensor embedded within the UKR bearing (*Figure 9*). The phase decreased to a median of -30 degrees at 10 Hz.

For reference purposes the amplitude transfer function and phase of the actuator load to actuator movement (Figure 10) are given, as well as the amplitude transfer function and phase of the actuator movement to capacitive change, all measured using the bearings with embedded sensors.

Harmonic distortion analysis showed that predominantly a second harmonic frequency was generated (dotted line *Figure 11*) with a median amplitude in the range of 5% of the first harmonic for the naked sensor, and 20% for the embedded sensor. Above 8 Hz only a first harmonic frequency was noted.

4 Discussion

This paper explored the feasibility of a capacitive load sensor embedded within the polyethylene bearing of a unicompartmental knee replacement. To our knowledge this has not previously been achieved. A flexible capacitive load sensor was developed that could be incorporated within the standard compression moulding manufacturing process of the Oxford UKR polyethylene bearing. Subsequent testing using a uniaxial servo-hydraulic material testing machine showed that the embedded sensor was capable of measuring forces within the polyethylene bearing.

It was demonstrated that adding diverging limbs in order to position the sensor within the mould tool (*Figure 3a*) was a simple and reliable way of centring the sensor within the bearing during manufacturing. The sensor was built using three layers of electrode, with the electrically driven electrode of the capacitor on both sides of the sensing electrode which was situated in the middle. This was done in order to isolate the sensing electrode from electromagnetic interference, similar to the use of extra shielding layers [33]. Using the driving electrodes instead of extra shielding resulted in the sensor being 35% thinner and more flexible. Additionally, adding extra layers adds manufacturing cost. Although the precise signal to noise ratio was not measured, there were no problems due to noise.

The development of a sensor which can be embedded within polyethylene represents a significant step towards the realization of an instrumented mobile UKR and to addressing the disadvantages of current instrumented implants. Our sensor was produced using commercially available construction methods and therefore the costs of manufacturing are lower compared to custom manufacturing. Furthermore, custom manufacturing methods often utilise 3D-printing, which uses polymers with a low melting temperature, and therefore would pose a major concern with respect to shape retention at the high temperatures and pressures [30] experienced during compressive

295 moulding. Polyamide is especially suited as a sensor because of its tolerance of high
296 temperatures [34]. The use of a flexible capacitive load sensor meant that the sensor could be
297 placed within the polyethylene bearing using the standard manufacturing process of polyethylene
298 bearings, offering significant additional cost advantages. Furthermore this also opens up the
299 possibility of load measurement in larger numbers of implants and different types of joint
300 replacement. The use of a sensor within the bearing reduces the complexity and the need for
301 moving parts compared to previous instrumented knees [8, 9]. In addition to the technological
302 advances described, there is the intra-operative benefit of the procedure remaining unchanged
303 as no additional bone resection would be required.

304

305 Viscous sensor response and pre-loading

306 The load sensor embedded in polyethylene exhibited a visco-elastic behaviour which prevented
307 traditional load measurement and calibration methods from being used. Instead, an initial static
308 load was required to achieve a quasi-steady state static sensor output; after which dynamic load
309 perturbations could be measured centred around the static load point. For the naked sensor foil,
310 polyimide, this pre-loading time was 10 seconds. The pre-loading compression curve showed that
311 for the polyimide foil, after reaching quasi steady state, beyond 90 seconds the confidence interval
312 increased (*Figure 6)*, potentially signifying capacitive drift. This behaviour was not observed in the
313 capacitive sensor embedded within the bearing.

314 Embedding the sensor in the UHMWPE bearing resulted in a quasi-static response only being
315 observed after 13 minutes under pre-load. The slower response compared to PI was probably
316 due to a number of factors. UHMWPE does not have a linear stress-strain curve, and exhibits a
317 time dependent stress-strain behaviour. Furthermore, the geometry of the bearing was not simple.
318 Manufacturing tolerances cause the concavity of the bearing to deviate from conformity with the

radius of the femoral component; thus it is preferred to have a smaller femoral component outer radius and a larger bearing internal radius. This is because if the bearing radius was smaller than that of the femoral component, there would be a perpendicular outwardly acting force within the bearing during compression, which could lead to edge loading and increased susceptibility to failure. Therefore, even in normal loading the highest load is concentrated at the centre of the bearing concavity, which then experiences a higher stress than the surrounding polyethylene. During the relaxation period prior to achieving quasi steady state, more and more of the load is distributed outwards from the centre of the concavity. This largely explains the longer pre-loading stage; it can be seen that initially the capacitance increases sharply, due to the concentrated load in the middle of the bearing where the sensor resides, but then as the UMPWHE compresses locally, the load spreads outwardly and the capacitance change lessens.

Previous literature has not referred to the viscous response of their sensor in detail [18-25, 33], although Laszczak *et al.* [33] possibly hinted at this based on the statement "*a specific tare load was applied to the sensor for 30 s… this strategy minimized a possible transient response resulting from the viscoelastic behaviour of the Elastomer*". Unfortunately, details about the tare load were not described, nor were details about the effectiveness of pre-loading in their experiment, making direct comparison to their results difficult.

Pre-loading in a practical scenario

Applying a pre-load for 13 minutes prior to measurement is a limitation. In practice, this could mean that before a physiological loading measurement can be recorded, a patient with an instrumented UKR should load the bearing by means of standing, walking, or running. We suspect that additional data could be obtained from experiments that do not feature pre-loading, but it would require a different calibration or more post-processing, which would need to be investigated further.

Calibration

Given that the range of temperatures the bearing will experienced in vivo is likely minimal given the tight self-regulation of temperature by the body, we do not expect problems due to temperature fluctuations. However this does needs to be investigated further. Additionally bearings would need to be individually calibrated prior to implantation. This would have to be done under pre-specified conditions and would also require further investigation.

Frequency Response

The tests showed that the compression response of the instrumented bearing to frequencies between 0.1 to 10 Hz was close to linear if a steady state pre-load corresponding to body mass was applied for at least 13 minutes prior to measurement.

The frequency response showed a low pass filter response, with a close to linear amplitude above -3 dB and up to 10 Hz. Therefore the sensor should be able to measure typical loading scenarios, such as gait where the predominant signal frequency is in the region of 1 Hz with a maximum signal content of 4.2 Hz [29]. Our findings suggest that the materials testing machine was not responsible for the observed low pass behaviour, given the constant phase we recorded between measured actuator load and actuator position (*Figure 10c*), whereas the phase change is introduced in (*Figure 10d*). Furthermore, our capacitance to digital converter measured at a frequency of 90 Hz, which ruled out its influence. We did observe characteristic low pass phase behaviour between actuator position (compression of the bearing) and capacitance increase, indicating that the sensor foil itself was causing low pass behaviour. Therefore, we ascribe this behaviour to the increasing incompressibility of the sensor foil construct, starting at frequencies above than 1 Hz.

Harmonic Frequency Generation

Harmonic frequency generation occurs as a result of a nonlinear load-strain relationship, and therefore, the output signal will have a different shape to the input signal. The measured second harmonic of 5% for the naked sensor foil was minimal and may be neglected, but a larger second order harmonic with an amplitude of 20% was observed in the embedded sensor which has the potential to be problematic. To what extent requires further investigation with actual physiological signals. A limitation was that above 8 Hz the method stopped working accurately; only the first harmonic was detected. This was most likely due to signal noise rather than the absence of second order frequency generation.

Sensitivity

A medium sensitivity of $6.1 * 10^{-17}$ F/N [99.3 % CI: $2.0 - 24$] was achieved, and a stress sensitivity of $4.5 * 10^{-17}$ F/MPa [99.3 % CI $1.5 - 18$]. The stress sensitivity that was obtained with the sensor was more than 44 times lower ($2 - 4 * 10^{-17}\ F/MPa$) than that of a comparable polyimide sensor [19] which had slots that allow for the polymer to expand more under compression with identical loads. Conversely, our sensor does not suffer from nonlinearity at lower loads.

Loading Magnitudes

In our study the peak load was 683 N. Using the 50-50 % load distribution between medial and lateral side of a knee [26-28], this equals a maximum load of 1366 N. In instrumented TKR, the peak force has ranged up to 4200 N [35]. Because of the use of sinusoidal waveforms required to measure frequency transfer characteristics of our sensor, we were limited to applying reduced peak loads. Further measurements are needed with gait loading patterns with equivalent loads to those measured using instrumented TKR [29].

Implant Development

Further development is required before a standalone embedded load sensor within a UKR can be used. The next step is that development of an embedded electronic system for recording and communication of data. Although communication with implanted sensors has been achieved before [8, 9], achieving this while at the same time meeting the requirements of being small enough to fit in a UKR bearing and being incorporated during the compression moulding process presents a significant challenge. The optimal positioning of a sensor and communication module within the bearing would need to be determined; we suggest this could initially be done with finite element based simulation, and subsequently using mechanical testing, before using the device *in-vivo.*

Also the potential use of such sensors in other implants using polyethylene bearings, such as total hip replacements, total knee replacements opens the scope of future applications. As these implants are larger, multiple sensors could be placed in a grid-like fashion, making it possible to measure load distribution and contact points.

5 Conclusion

We have developed a novel capacitive load sensor that can be embedded in UKR bearings, and potentially other joint replacement bearings, using standard production methods, and have assessed its dynamic sensitivity, frequency response and nonlinear distortion. We found that to obtain repeatable results, the instrumented bearing has to be pre-loaded for 13 minutes. The requirement for pre-loading was not due to the sensor but was a manifestation of the complex viscous-elastic behaviour of the UHMWPE component. After pre-loading there was a linear response to superimposed dynamic loading frequencies, with a low pass filter characteristic with a -3 dB frequency of 10 Hz. Each sensor had dimensions of 2x2 mm, a median load sensitivity of 6.1* 〖10〗^(-17) F/N [99.3% CI: 0.67-8], and a median stress sensitivity of 4.5* 〖10〗^(-17)

F/MPa [99.3 % CI: 1.5-18]. We conclude the sensor could be used to measure physiological loads, spanning the physiological frequency range.

Figures

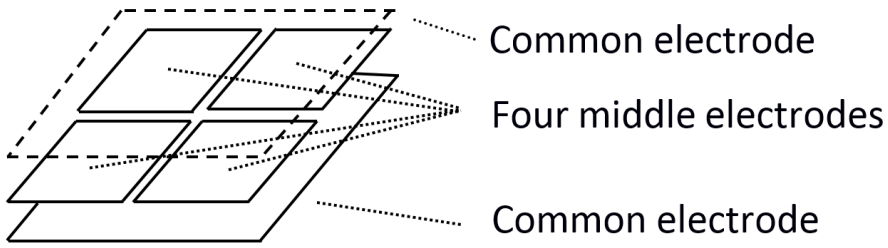

Figure 1: *Illustration showing the layout of the common and middle electrodes, made of a layer of solid copper foil*

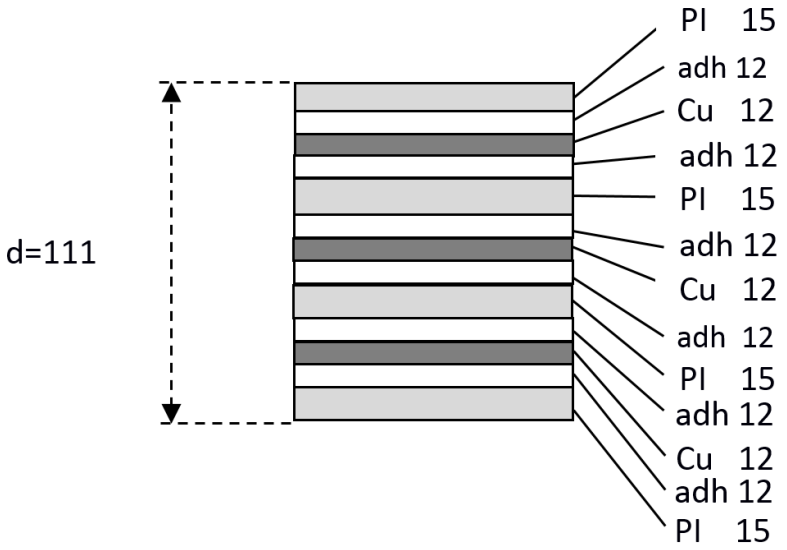

Figure 2: *Illustration showing the composition of the capacitive sensor layers, where PI = Polyimide, adh = adhesive, Cu = copper. For each layer, the thickness is given in micrometers (µm).*

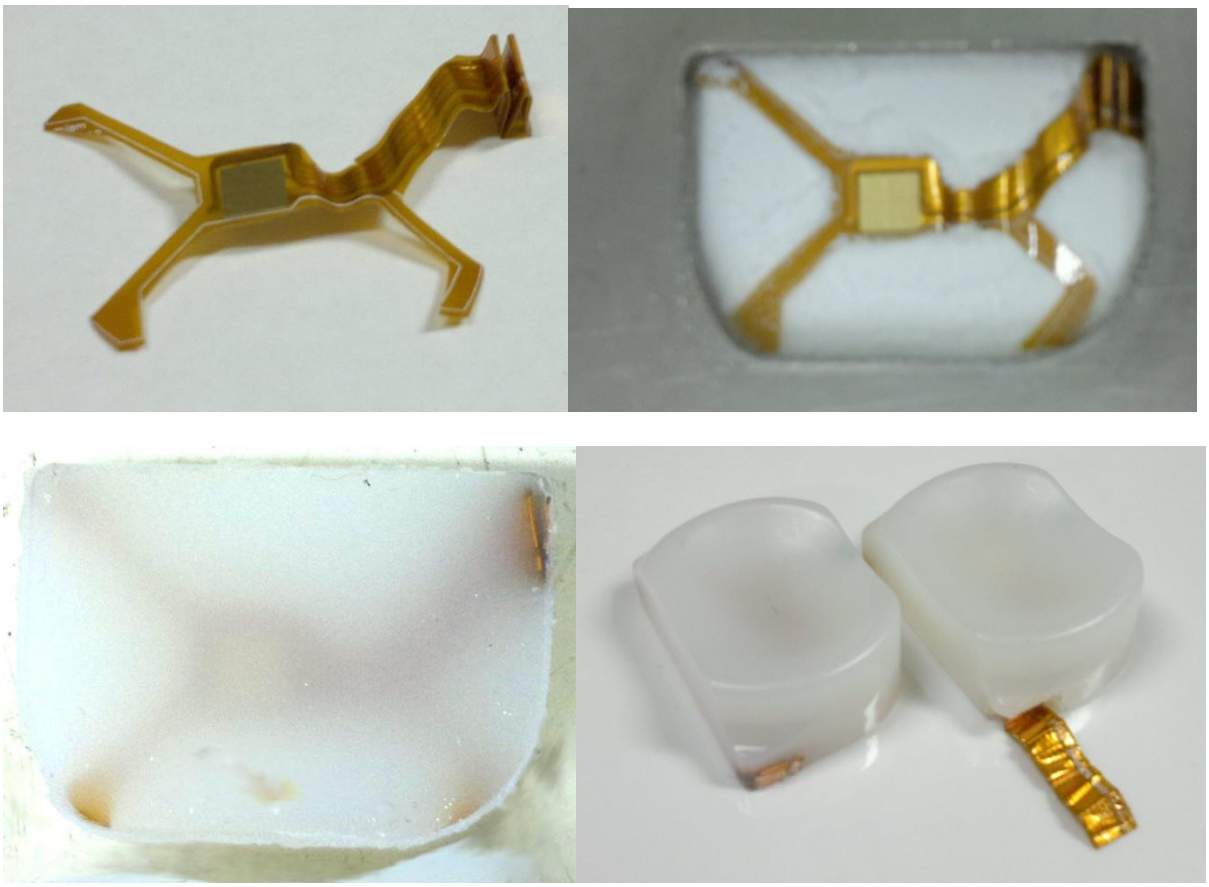

Figure 3: *(a) (top left) the sensor assembly with the capacitive sensors in the middle, and three extending legs for centring the sensor within the mould. The sensor leads were folded in a harmonica fold. (b) (top right) The sensor within the mould on half of the UHMWPE powder. (c) (bottom left) the moulded UKR bearing with the embedded sensor. (d) (bottom right) the folded sensor leads were recovered with a hot cutting tool and unfolded.*

NOTE TO EDITOR: WE ARE EXPECTING THAT YOU PREFER TO ADD THE INDIVIDUAL LABELS YOURSELF. If not, please contact us and we'll add (a),(b),etc.

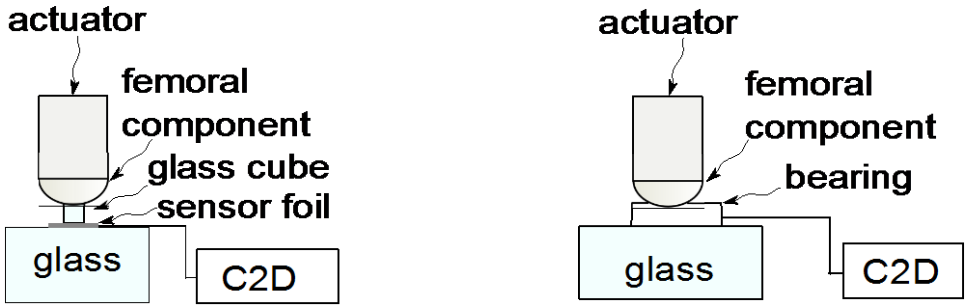

Figure 4: *(a)(left) Diagram of the servo-hydraulic loading rig setup, showing hydraulic actuator, femoral component, sensor foil, bearing, glass base, and C2D (capacitance to digital converter), and (b)(right) the identical setup but testing a bearing sample.*

NOTE TO EDITOR: WE ARE EXPECTING THAT YOU PREFER TO ADD THE INDIVIDUAL LABELS YOURSELF. If not, please contact us and we'll add (a),(b),etc.

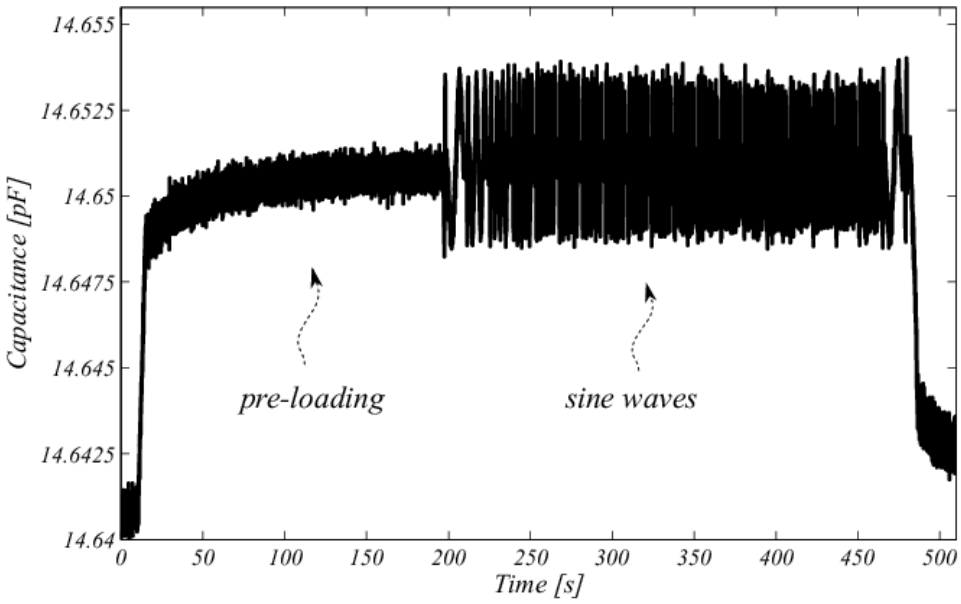

Figure 5: *Plot of capacitance vs. time for a full measurement cycle of an instrumented bearing. The sinusoidal loads are 10 seconds each of 0.1 Hz up to 1 Hz in steps of 0.1 Hz, and 1 Hz to 10 Hz in steps of 1 Hz, with ±293 N amplitude.*

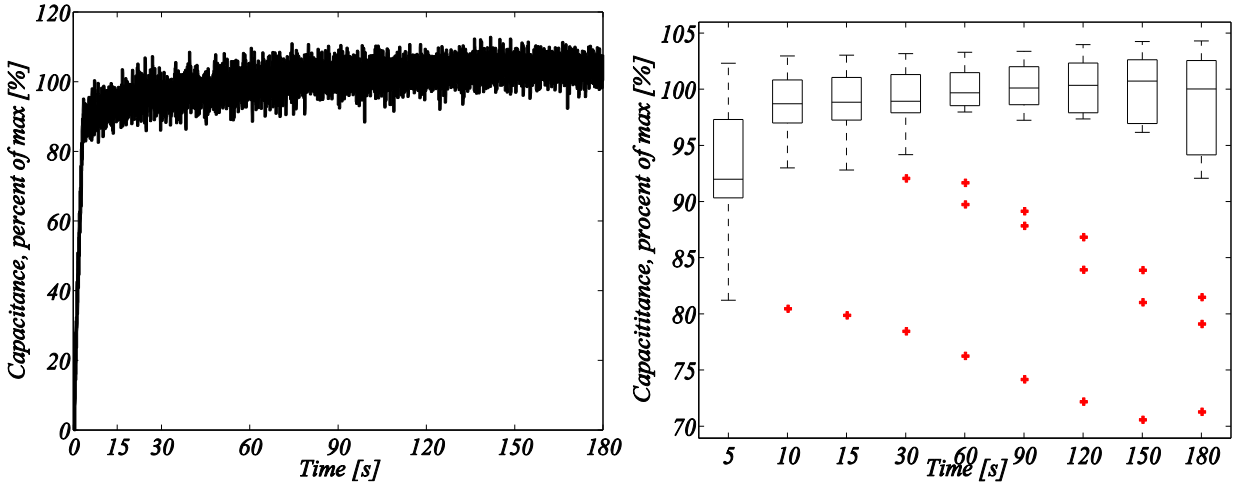

Figure 6: *Plots showing capacitance against time for pre-loading of the naked sensors. The raw data of a single sample is illustrated in (a)(left) and (b)(right) an overview of results for all 5 samples with 5 repeats per sample (25 in total). No load equals 0 % and maximum median capacitance equals 100 %, Note that greater than 95 % of the steady-state value was reached within 10 seconds. The red data points are the outliers of the distribution shown by each box plot. NOTE TO EDITOR: WE ARE EXPECTING THAT YOU PREFER TO ADD THE INDIVIDUAL LABELS YOURSELF. If not, please contact us and we'll add (a),(b),etc.*

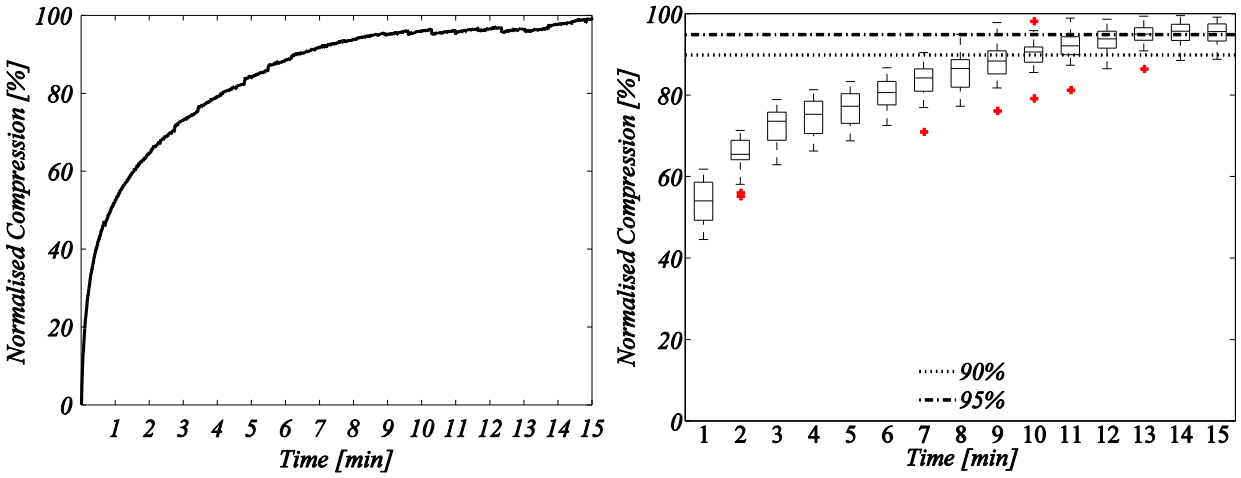

Figure 7: *Plots showing capacitance against time for pre-loading of the instrumented sensors. The raw data of a single sample is illustrated in (a) (left) and an overview of results for all samples in (b) (right). Note that greater than 95 % of the steady-state value was reached within 13 minutes. The red data points are the outliers of the distribution shown by each box plot.*

NOTE TO EDITOR: WE ARE EXPECTING THAT YOU PREFER TO ADD THE INDIVIDUAL LABELS YOURSELF. If not, please contact us and we'll add (a),(b),etc.

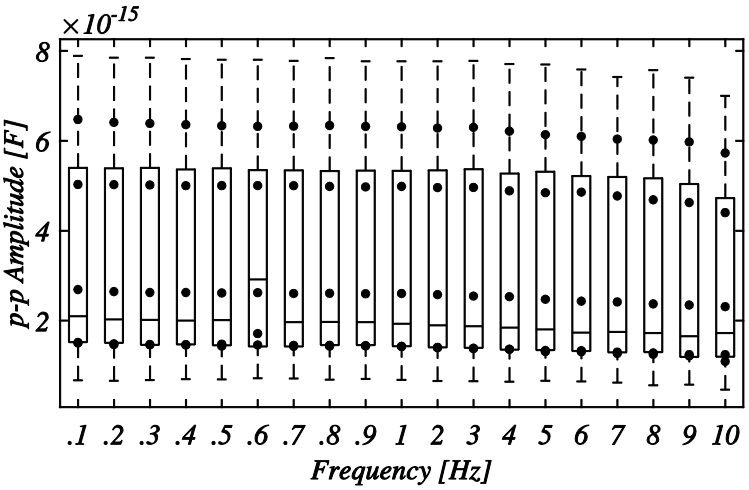

475

476 ***Figure 8:*** *Normalised amplitude (peak to peak) capacitive change of the bare sensor foil for 33 N*
477 *sinusoidal loading, based on 5 sensors for a total of 25 measurements. The 99.3% CI typically*
478 *lies between 0.67 and 8 fF. The black dots represent the means of each individual sensor foil (5*
479 *experiments each). The results of two measurements, below 2, partially overlap.*

480

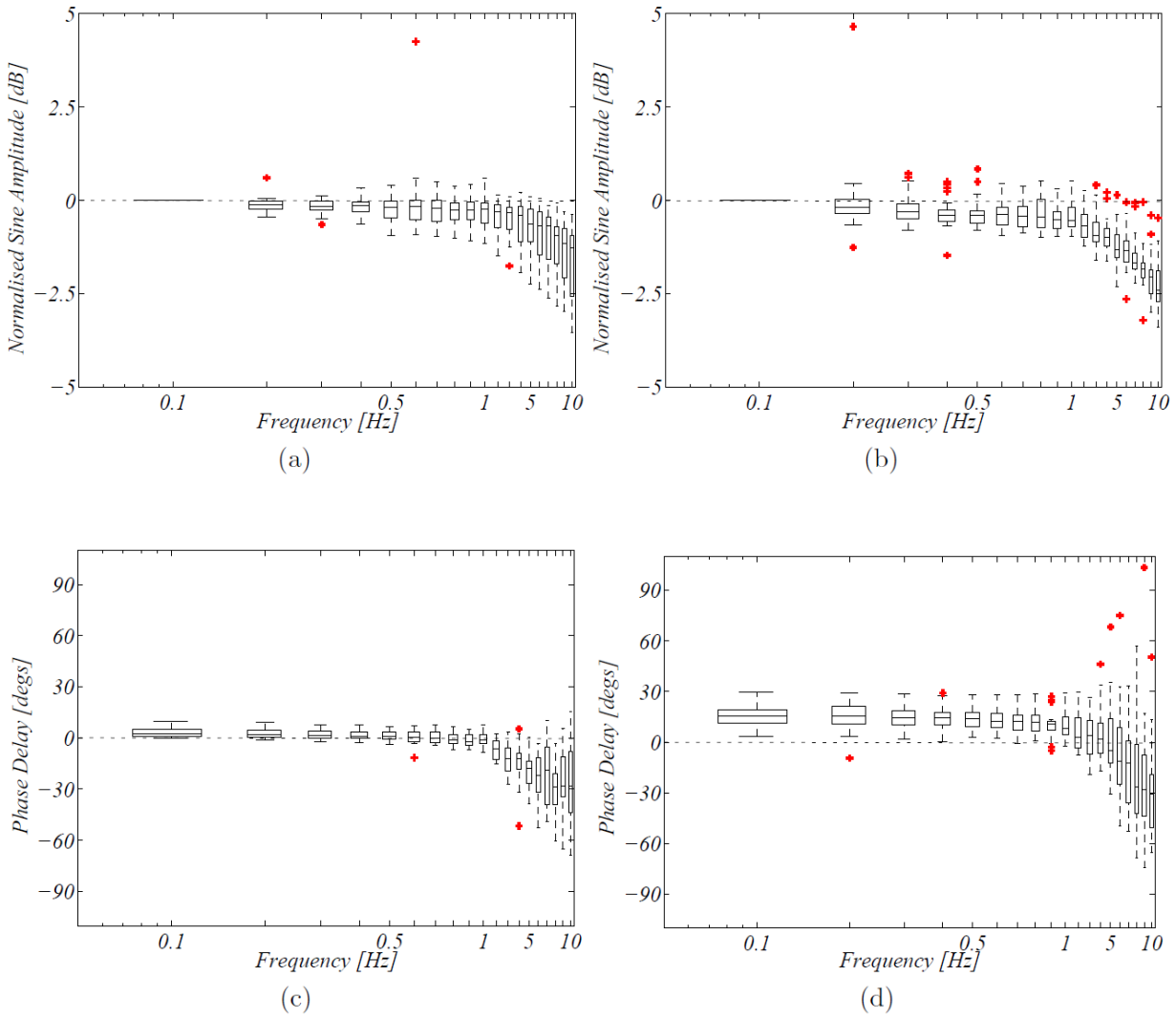

Figure 9: *Normalised load to capacitance amplitude frequency transfer response for the (a)(top left) naked sensor foil, and (b)(top right) sensor embedded within the bearing, and the phase responses for (c)(bottom left) the naked sensor foil and (d)(bottom right) the sensor embedded within the bearing. The red points are outliers as of a result of showing the distribution as a boxplot.*

NOTE TO EDITOR: WE ARE EXPECTING THAT YOU PREFER TO ADD THE INDIVIDUAL LABELS YOURSELF. If not, please contact us and we'll add (a),(b),etc.

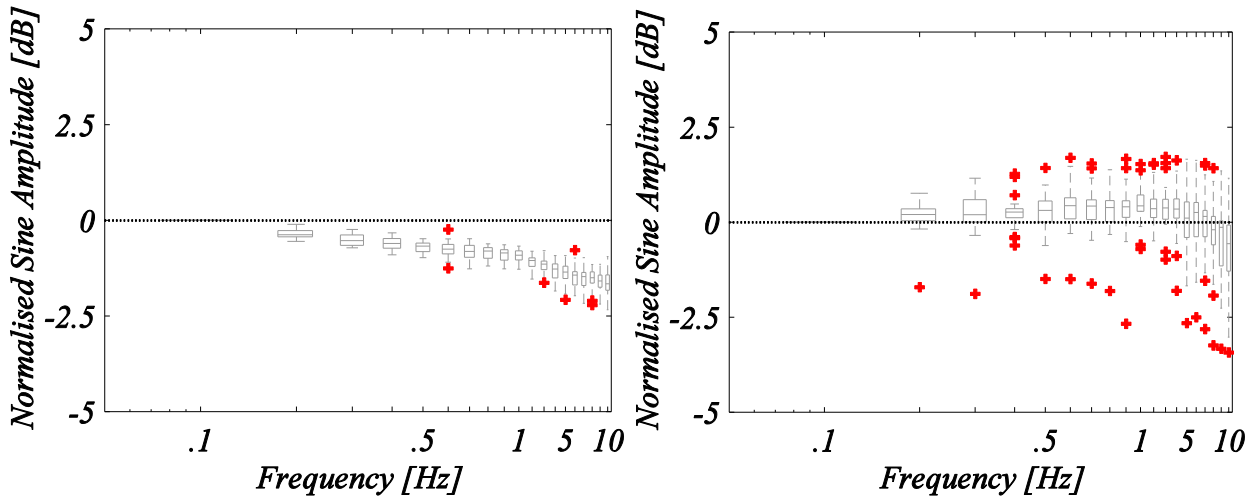

(a) (b)

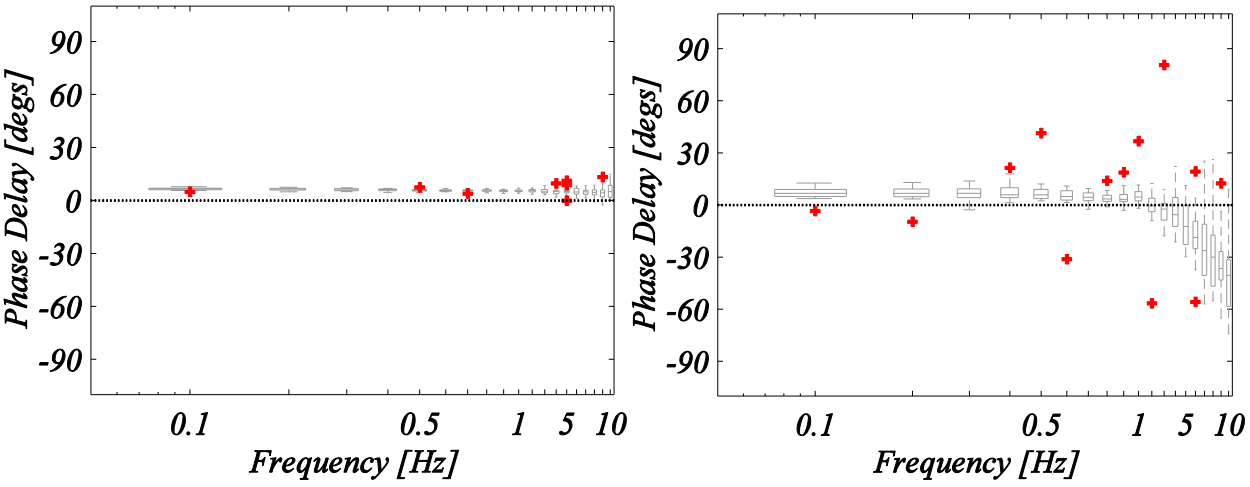

(c) (d)

Figure 10: (a *Normalised load to actuator position amplitude frequency transfer response, (b) normalised actuator position to capacitance frequency transfer response, (c) load to actuator position phase response, and (d) actuator position to capacitance change phase response, all for the sensor embedded within the bearing. The red points are outliers as of a result of showing the distributions as a boxplot.*

NOTE TO EDITOR: WE ARE EXPECTING THAT YOU PREFER TO ADD THE INDIVIDUAL LABELS YOURSELF. If not, please contact us and we'll add (a),(b),etc.

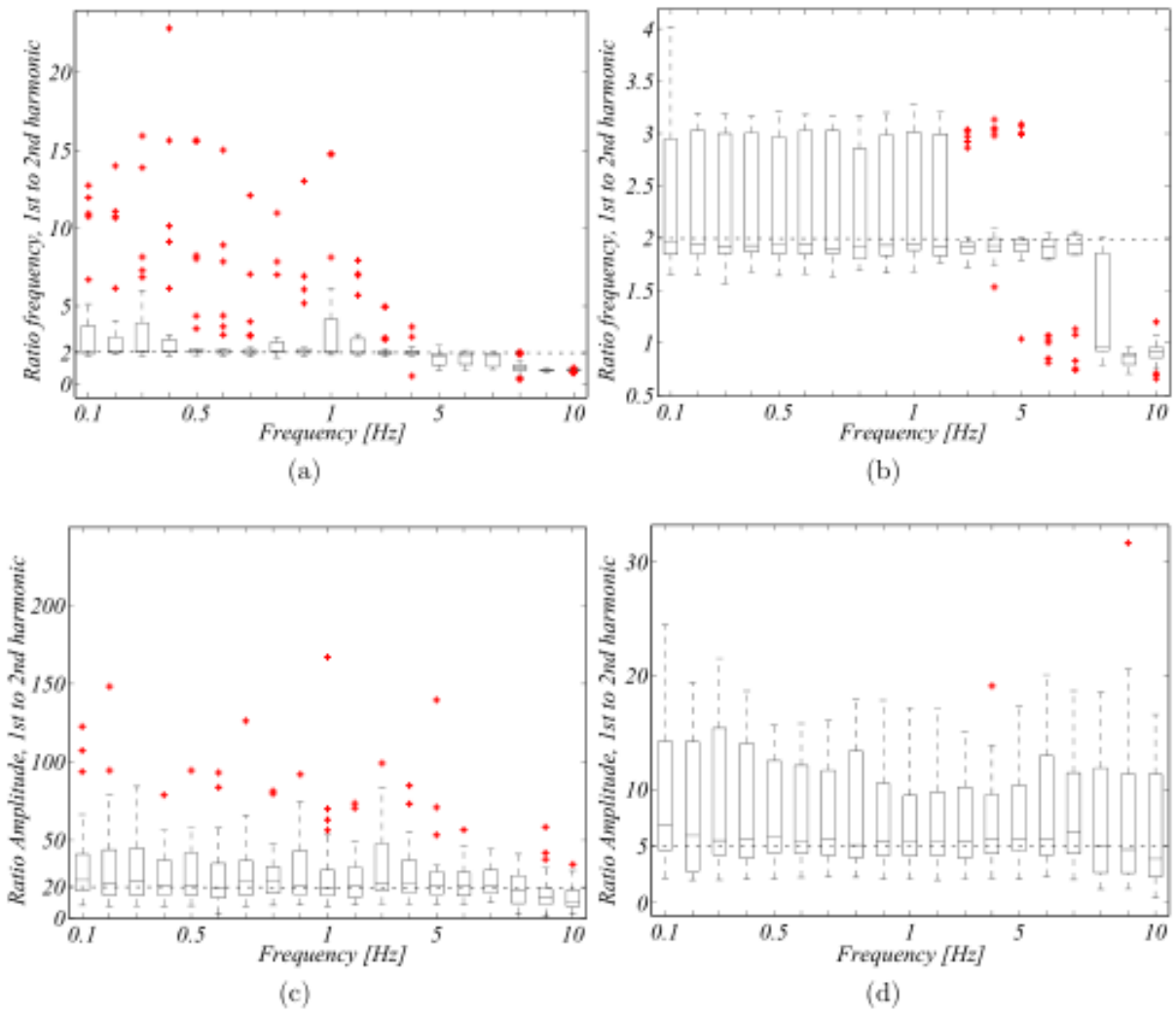

Figure 11: *Results for the dual sine wave fitting: the ratio of the first to the second harmonic frequency (a) the naked sensor and (b) the embedded sensor and the ratio of the amplitudes for (c) the naked sensor and (d) the embedded sensor. The dotted trace shows the best fit to the means of the distributions. The red points are outliers as of a result of showing the distribution as a boxplot.*

NOTE TO EDITOR: WE ARE EXPECTING THAT YOU PREFER TO ADD THE INDIVIDUAL LABELS YOURSELF. If not, please contact us and we'll add (a),(b),etc.

References

1. Griffin, T.M. and F. Guilak, *The Role of Mechanical Loading in the Onset and Progression of Osteoarthritis.* Exercise and Sport Sciences Reviews, 2005. **33**(4): p. 195-200.
2. Radin, E.L., I.L. Paul, and R.M. Rose, *Role of mechanical factors in pathogenesis of primary osteoarthritis.* the Lancet, 1972. **299**(7749): p. 519-522.
3. Meyer, A.J., et al., *Are external knee load and EMG measures accurate indicators of internal knee contact forces during gait?* J Orthop Res, 2013. **31**(6): p. 921-9.
4. Walker, P.S., et al., *Preclinical evaluation method for total knees designed to restore normal knee mechanics.* J Arthroplasty, 2011. **26**(1): p. 152-60.
5. Wehner, T., L. Claes, and U. Simon, *Internal loads in the human tibia during gait.* Clin Biomech (Bristol, Avon), 2009. **24**(3): p. 299-302.
6. Fregly, B.J., et al., *Sensitivity of knee replacement contact calculations to kinematic measurement errors.* J Orthop Res, 2008. **26**(9): p. 1173-9.

7. D'Lima, D.D., et al., *In vivo contact stresses during activities of daily living after knee arthroplasty.* J Orthop Res, 2008. **26**(12): p. 1549-55.
8. D'Lima, D.D., et al., *An implantable telemetry device to measure intra-articular tibial forces.* J Biomech, 2005. **38**(2): p. 299-304.
9. Heinlein, B., et al., *Design, calibration and pre-clinical testing of an instrumented tibial tray.* J Biomech, 2007. **40 Suppl 1**: p. S4-10.
10. Price, A.J., et al., *Simultaneous in vitro measurement of patellofemoral kinematics and forces following oxford medial unicompartmental knee replacement.* J Bone Joint Surg [Br], 2006. **88-B**: p. 1591-5.
11. Pandit, H., et al., *Combined anterior cruciate reconstruction and Oxford unicompartmental knee arthroplasty: in vivo kinematics.* Knee, 2008. **15**(2): p. 101-6.
12. Patil, S., et al., *Can normal knee kinematics be restored with unicompartmental knee replacement?* J Bone Joint Surg Am, 2005. **87**(2): p. 332-8.
13. Price, A.J., et al., *Sagittal plane kinematics of a mobile-bearing unicompartmental knee arthroplasty at 10 years.* The Journal of Arthroplasty, 2004. **19**(5): p. 590-597.
14. Robinson, B.J., et al., *A kinematic study of lateral unicompartmental arthroplasty.* The Knee, 2002. **9**(3): p. 237-40.
15. Yang, K.Y., et al., *Minimally invasive uniondylar versus total condylar knee arthroplasty - early results of a matched-pair comparison.* Singapore Med, 2003. **44**(11): p. 559-62.
16. Pegg, E.C., et al., *Fracture of mobile unicompartmental knee bearings: a parametric finite element study.* Proc Inst Mech Eng H, 2013. **227**(11): p. 1213-23.
17. Micro-measurements, V., in *Strain gage selection - criteria, procedures, recommendations*. 2005: http://www.vishaypg.com/docs/11055/tn505.pdf. p. 1-16.
18. Dobrzynska, J.A. and M.A.M. Gijs, *Capacitive flexible force sensor.* Procedia Engineering, 2010. **5**: p. 404-407.
19. Dobrzynska, J.A. and M.A.M. Gijs, *Flexible polyimide-based force sensor.* Sensors and Actuators A: Physical, 2012. **173**(1): p. 127-135.
20. Cheng, M.Y., C.L. Lin, and Y.J. Yang, *Tactile and shear stress sensing array using capacitive mechanisms with floating electrodes*, in *Micro Electro Mechanical Systems (MEMS)*. 2010, IEEE.
21. Kim, B.-C., et al., *Multi-axis Flexible Force Sensor for Tactile Display*, in *Sensors*. 2011. p. 1453-6.
22. Lee, H.-K., et al., *Normal and Shear Force Measurement Using a Flexible Polymer Tactile Sensor With Embedded Multiple Capacitors.* Journal of Microelectromechanical Systems, 2008. **17**(4): p. 934-942.

23. Surapeneni, R., et al., *A highly sensitive flexible pressure and shear sensor array for measurement of ground reactions in pedestrian navigation* in *Solid-State sensors, Actuators and Microsystems Conference (TRANSDUCERS)*. 2011. p. 906-9.
24. Valdastri, P., et al., *Characterization of a novel hybrid silicon three-axial force sensor.* Sensors and Actuators A: Physical, 2005. **123-124**: p. 249-257.
25. da Rocha, J.G.V., P.F.A. da Rocha, and S. Lanceros-Mendez, *Capacitive Sensor for Three-Axis Force Measurements and Its Readout Electronics.* IEEE Transactions on Instrumentation and Measurement, 2009. **58**(8): p. 2830-2836.
26. Varadarajan, K.M., et al., *In vivo contact kinematics and contact forces of the knee after total knee arthroplasty during dynamic weight-bearing activities.* J Biomech, 2008. **41**(10): p. 2159-68.
27. D'Lima, D.D., et al., *Tibial forces measured in vivo after total knee arthroplasty.* J Arthroplasty, 2006. **21**(2): p. 255-62.
28. Johnson, F., S. Leitl, and W. Waugh, *The distribution of load across the knee, a comparison of static and dynamic measurements.* Bone and Joint Surgery, 1980. **62-B**: p. 346-9.
29. *www.orthoload.com*. 2012; datasets K1L11018_80p_gait and k2l_290409_1_109p].
30. Kurtz, S.M., *The UHMWPE Handbook, Ultra-High Molecular Weight Polyethylene in Total Joint Replacement*. 2004.
31. ISO, *ISO Standard 376:2011 Metallic materials -- calibration of force-proving instruments used for the verification of uniaxial testing machines*. 2011.
32. Meyer, R.W. and L.A. Pruitt, *The effect of cyclic true strain on the morphology, structure, and Relaxation behavior of ultra high molecular weight polyethylene* Polymer, 2001. **42**(12): p. 5293-5306.
33. Laszczak, P., et al., *Development and validation of a 3D-printed interfacial stress sensor for prosthetic applications.* Med Eng Phys, 2015. **37**(1): p. 132-7.
34. Khazaka, M.L., et al., *Effects of mechanical stress, thickness and atmosphere on ageing of polyimide thin films at high temperature.* Polymer Degradation and Stability, 2013. **98**: p. 361-7.
35. Bergmann, G., et al., *Standardized Loads Acting in Knee Implants.* PLOS ONE, 2014. **9**(1): p. e86035.